A fourth-order accurate difference approximation for the incompressible Navier-Stokes equations

William D. Henshaw
IBM Research Division
Thomas J. Watson Research Centre
Yorktown Heights, NY 10598

Heinz-Otto Kreiss
Department of Mathematics
University of California at Los Angeles
Los Angeles, CA 90025

Luis G. M. Reyna
IBM Research Division
Thomas J. Watson Research Centre
Yorktown Heights, NY 10598

This article appeared in Computers and Fluids, **23**, number 4, pages 575–593, 1994.

Abstract: We discuss fourth-order accurate difference approximations for parabolic systems and for the incompressible Navier-Stokes equations. A general principle for deriving numerical boundary conditions for higher-order accurate difference schemes is described. Some difference approximations for parabolic systems are analyzed for stability and accuracy. The principle is used to derive stable and accurate numerical boundary conditions for the incompressible Navier-Stokes equations. Numerical results are given from a fourth-order accurate scheme for the incompressible Navier-Stokes equations on overlapping grids in two and three-space dimensions.

Dedication: To Egon Krause on the occasion of his sixtieth birthday.

1 Introduction

The advantages of using higher-order accurate methods for the numerical solution of partial differential equations are by now well known. For problems with periodic boundary conditions, for example, spectral methods are widely used. Higher-order difference methods, such as the fourth-order methods discussed here, also offer significant advantages over lower-order schemes.

Applying a high-order method on a complicated region is a difficult task. One major difficulty is the generation of a grid for the region. The grid must be smooth enough so that errors associated with variations in the grid do not over-whelm the errors in the method. To generate a grid we advocate the method of overlapping grids, [1], whereby a smooth grid can be created on a complicated region.

A second difficulty associated with applying higher-order difference methods is the choice of numerical boundary conditions. Some care is required in differencing the equations near the boundary so that the resulting scheme remains accurate and stable. Fortunately, with an overlapping grid, the mesh can be constructed so that the grid lines follow the boundary. This feature, which is clearly useful from a practical point of view is also important for theoretical reasons because this means that the stability and accuracy analysis can be reduced to the study of a constant coefficient half-plane problem. With recent advances and simplifications in the stability and accuracy analysis one may say that the treatment of this latter problem is quite well understood.

In this paper we discuss a general principle for deriving numerical boundary conditions for fourth-order difference methods. The basic idea is (1) use the interior equation on the boundary and (2) apply the boundary condition operator to the interior equation and use the resulting equation to lower order on the boundary. We use this principle to derive boundary conditions for parabolic systems and for the incompressible Navier-Stokes equations. We describe a computer program that has been written to solve the incompressible Navier-Stokes equations in general two and three dimensional domains using overlapping grids.

We begin, in Section 2, by discussing well-posed problems. The concept of well-posedness of a continuous problem is closely related to the stability of the corresponding discrete problem. In Section 3 we consider the stability and accuracy of fourth-order accurate difference approximations of parabolic systems and present a principle for deriving extra numerical boundary conditions. In Section 4 we study the incompressible Navier-Stokes equations. We analyze the well-posedness of a half plane problem and the stability of a fourth-order accurate difference approximation. Finally in Section 5 we present some results from the numerical solution of the incompressible equations on overlapping grids that demonstrate the accuracy of the method.

2 Well-posed problems

In this section we review some results concerning well-posed initial boundary value problems. The interested reader should refer to [4][6], for example, for further details. Consider the initial boundary value problem for a quasilinear parabolic system of partial differential equations on a general time-space domain $[0,T]\times\Omega$:

$$\begin{aligned} \mathbf{u}_t &= P(\mathbf{x},t,\mathbf{u},\partial/\partial\mathbf{x})\mathbf{u}+\mathbf{F}(\mathbf{x},t), && \mathbf{x}\in\Omega \\ B(\mathbf{u}) &= \mathbf{g}, && \mathbf{x}\in\partial\Omega \\ \mathbf{u}(\mathbf{x},0) &= \mathbf{f}(\mathbf{x}), \\ P &:= \sum_\nu A_\nu(\mathbf{x},t,\mathbf{u})\frac{\partial^{|\nu|}}{\partial x_1^{\nu_1}\cdots\partial x_s^{\nu_s}} \ . \end{aligned}$$

In Kreiss and Lorenz [4] it was shown how to reduce this problem to a half-space problem for systems with constant coefficients. We therefore consider a parabolic system in two-space dimensions

$$\mathbf{u}_t = A_{11}\mathbf{u}_{xx}+A_{22}\mathbf{u}_{yy}+A_{10}\mathbf{u}_x+A_{02}\mathbf{u}_y+A_{00}\mathbf{u}+\mathbf{F} := L\mathbf{u}+\mathbf{F} \tag{1}$$

of n equations with constant coefficients on the halfspace $0\le x<\infty,\ -\infty<y<\infty,\ t\ge 0$. At $t=0$ we give initial conditions

$$\mathbf{u}(x,y,0)=\mathbf{f}(x,y), \tag{2}$$

and at $x=0$ we give n linearly independent boundary conditions

$$B_0\mathbf{u}(0,y,t)+B_1\mathbf{u}_x(0,y,t)=\mathbf{g}(y,t). \tag{3}$$

We also assume that all functions are 2π-periodic in y. Define

$$\mathbf{u}=(u_1,\ldots,u_n)^T \quad , \quad \langle\mathbf{u},\mathbf{v}\rangle=\sum_\mu u_\mu^* v_\mu \quad , \quad |\mathbf{u}|^2=\langle\mathbf{u},\mathbf{u}\rangle \quad ,$$

and let

$$(\mathbf{u},\mathbf{v}) = \int_0^\infty \int_0^{2\pi} \langle \mathbf{u},\mathbf{v}\rangle dx dy, \quad \|\mathbf{u}\|^2 = (\mathbf{u},\mathbf{u})$$

denote the usual L_2-scalar product and norm.

Definition 1 *The problem (1)–(3) is well-posed in the generalized sense if there are constants α, K such that, for all $\eta \geq \alpha$, the solutions of (1)–(3) satisfy the estimate*

$$\int_0^\infty e^{-\eta t}(\|\mathbf{u}\|^2 + \|\mathbf{u}_x\|^2)dt \leq K\left(\int_0^\infty (\|\mathbf{F}\|^2 + |\mathbf{g}|_\Gamma^2)dt + \|\mathbf{f}\|^2\right), \tag{4}$$

where

$$|\mathbf{g}|_\Gamma^2 = \int_0^{2\pi} |\mathbf{g}(y,t)|^2 dy.$$

Two important results in the theory, which we state but do not prove here, are contained in the following two theorems

Theorem 1 *The general estimate (4) holds, if and only if, it holds for the particular case where $\mathbf{F} \equiv \mathbf{f} \equiv \mathbf{0}$.*

Theorem 2 *The lower order terms $A_{10}\mathbf{u}_x + A_{02}\mathbf{u}_y + A_{00}\mathbf{u}$ have no influence on the well-posedness and can be neglected.*

Thus, we need only consider the following constant coefficient parabolic problem,

$$\begin{cases} \mathbf{u}_t = A_1\mathbf{u}_{xx} + A_2\mathbf{u}_{yy} \\ \mathbf{u}(x,y,0) = 0 \\ B_0\mathbf{u}(0,y,t) + B_1\mathbf{u}_x(0,y,t) = \mathbf{g}(y,t) \ . \end{cases} \tag{5}$$

Recall that the Fourier transform and inverse of a 2π-periodic function $f(y) = f(y+2\pi)$ are defined by

$$f(y) = \sum_{n=-\infty}^{\infty} \bar{f}(\omega_n)e^{i\omega_n y} \quad , \quad \bar{f}(\omega_n) = \frac{1}{2\pi}\int_0^{2\pi} e^{-i\omega_n y}f(y)dy \quad , \quad \omega_n = n$$

while the Laplace transform and inverse of a function $f(t)$, (where $|f(t)|<e^{\gamma t}$ as $t \to \infty$) are

$$\tilde{f}(s) = \int_0^\infty e^{-st}f(t)dt \quad , \quad f(t) = \frac{1}{2\pi i}\int_{\gamma-i\infty}^{\gamma+i\infty} e^{st}\tilde{f}(s)ds.$$

We solve the problem (5) by Fourier transforming it in y and Laplace transforming it in t, obtaining the following equation for the transformed variable $\hat{\mathbf{u}} = \hat{\mathbf{u}}(x,\omega,s)$,

$$s\hat{\mathbf{u}} = A_1\hat{\mathbf{u}}_{xx} - \omega^2 A_2\hat{\mathbf{u}}, \quad 0 < x < \infty, \tag{6}$$

$$B_0\hat{\mathbf{u}} + B_1\hat{\mathbf{u}}_x = \hat{\mathbf{g}}. \tag{7}$$

Define

$$\|\hat{\mathbf{u}}\|_x^2 := \int_0^\infty |\hat{\mathbf{u}}|^2 dx \ .$$

By Parseval's relation it follows that

Theorem 3 *The problem is well-posed in the generalized sense (that is an estimate of the form (4) holds), if and only if, the solutions of (6),(7) satisfy the estimate*

$$\|\hat{\mathbf{u}}\|_x^2 + \|\hat{\mathbf{u}}_x\|_x^2 \leq K|\hat{\mathbf{g}}|^2 \ ,$$

for all ω and all $Re(s) \geq \alpha$.

Equation (6) is a system of ordinary differential equations. Its general solution, belonging to L_2, is of the form

$$\hat{\mathbf{u}} = \sum_{j=1}^{n} \sigma_j e^{\lambda_j x} \mathbf{w}_j, \tag{8}$$

where $Re(\lambda_j) < 0$ for $Re(s) > 0$. Here $\lambda_j = \lambda_j(\omega, s)$ and $\mathbf{w}_j = \mathbf{w}_j(\omega, s)$ are solutions of

$$\big((sI + \omega^2 A_2) - A_1 \lambda^2\big)\mathbf{w} = 0,$$

with $\|\mathbf{w}\|_x = 1$. It can be shown that there are exactly n linearly independent solutions.

Substituting (8) into the boundary conditions gives us a linear system of equations for $\boldsymbol{\sigma} = (\sigma_1, \ldots, \sigma_n)^T$

$$\mathcal{B}\boldsymbol{\sigma} = \hat{\mathbf{g}}. \tag{9}$$

Therefore, we have

Theorem 4 *The problem (5) is well-posed in the generalized sense if, and only if, there is are constants K_1 and α, such that, for all ω and all s with* $\mathrm{Re}(s) > \alpha$,

$$|\boldsymbol{\sigma}| \leq K_1 |\hat{\mathbf{g}}|. \tag{10}$$

Theorem 4 defines a condition for well-posedness that can be more easily verified than the condition that appears in the original definition. In the next section we determine the analogous result for the the discretized form of the equations.

3 Stability and numerical boundary conditions

We now study the discrete version of the problem. Since all difficulties occur in the direction normal to the boundary, it will simplify the presentation if we only discretize in the x-direction and keep the y-direction continuous. We introduce a mesh spacing h and a grid in the x-direction, $G = \{x_\nu = \nu h\ ,\ \nu = -2, -1, 0, 1, 2, \ldots\}$. The grid will include two extra fictitous (ghost) points outside the computation domain. Let $\mathbf{v}_\nu(y,t)$ denote the discrete approximation to $\mathbf{u}(x_\nu, y, t)$.

We approximate the parabolic system (1)–(3) by a semi-discrete difference method of the form

$$\begin{cases} \partial_t \mathbf{v}_\nu = L_h \mathbf{v}_\nu + F(x_\nu, y, t), & \nu = 1, 2, 3, \ldots, \\ \mathbf{v}_\nu(y, 0) = \mathbf{f}(x_\nu, y), & \nu = -2, -1, 0, 1, 2, 3, \ldots \\ B_0 \mathbf{v}_0(y,t) + B_1 D_h \mathbf{v}_0(y,t) = \mathbf{g}^I(y,t) & \\ B_{2h}\mathbf{v}_0 = \mathbf{g}^{II}(y,t)\ . & \end{cases} \tag{11}$$

Here L_h is a difference approximation for L, D_h is a difference approximation for $\partial/\partial x$ while $B_{2h}\mathbf{v}_0 = \mathbf{g}^{II}$ are additional numerical boundary conditions. We will discuss the choice of these conditions shortly. We abuse the notation by writing $B_0\mathbf{v}_0$ to mean $B_0\mathbf{v}_\nu$ evaluated at $\nu = 0$.

Instead of the L_2-norm, we now use a discrete norm $\|\mathbf{v}(\cdot,t)\|_h$ (for our purposes here it will not be necessary to explicity define this discrete norm). We now define

Definition 2 *The problem (11) is stable if there are constants α, K and h_0, such that, for all $\eta \geq \alpha$ and all $h < h_0$, the solutions of (11) satisfy the estimate (4) where the L_2-norms are replaced by discrete norms.*

Theorems 1-3 are also valid in the discrete case. Therefore, we need only consider approximations for the parabolic system (5), where the lower order terms have been dropped. Let $E\mathbf{v}_\nu = \mathbf{v}_{\nu+1}$ denote the translation operator in the x-direction. Define the difference operators

$$\begin{aligned} hD_+ &= E - I, \quad hD_- = I - E^{-1}, \\ h^2 D_+ D_- &= E - 2I + E^{-1}, \quad \Delta_h = D_+D_-(I - \frac{h^2}{12}D_+D_-), \\ 2hD_0 &= E - E^{-1}, \quad D_h = D_0(I - \frac{h^2}{6}D_+D_-). \end{aligned}$$

D_0 and D_h are the usual second and fourth-order accurate difference approximations to $\partial/\partial x$, while D_+D_- and Δ_h approximate $\partial^2/\partial x^2$ to second and fourth-order accuracy, respectively. The semi-discrete approximation is

$$\partial_t \mathbf{v}_\nu = A_1 \Delta_h \mathbf{v}_\nu + A_2 \partial_y^2 \mathbf{v}_\nu, \quad \nu = 1, 2, 3, \dots \tag{12}$$
$$\mathbf{v}_\nu(y, 0) = 0, \quad \nu = -2, -1, 0, 1, 2, \dots \tag{13}$$
$$B_0 \mathbf{v}_0(y, t) + B_1 D_h \mathbf{v}_0(y, t) = \mathbf{g}^I(y, t), \tag{14}$$
$$B_{2h} \mathbf{v}_0 = \mathbf{g}^{II}(y, t). \tag{15}$$

To completely specify the approximation we need to define the scheme near the boundary. We require $2n$ conditions to express $\mathbf{v}_{-2}(y, t)$ and $\mathbf{v}_{-1}(y, t)$ in terms of $\mathbf{v}_0(y, t), \mathbf{v}_1(y, t), \dots$

A principle for deriving numerical boundary conditions: The basic idea for deriving numerical boundary conditions is as follows. The continuous problem is of the form

$$\begin{cases} \mathbf{u}_t = L\mathbf{u} + \mathbf{F} & \text{for } x > 0 \\ B\mathbf{u}(0, y, t) := B_0 \mathbf{u}(0, y, t) + B_1 \mathbf{u}_x(0, y, t) = \mathbf{g}(y, t) & \end{cases} \tag{16}$$

Applying the boundary condition operator B to the equation gives

$$(B\mathbf{u})_t = (BL)\mathbf{u} + B\mathbf{F} \ ,$$

and thus the following equation holds on the boundary:

$$(BL)\mathbf{u}(0, y, t) = \mathbf{g}_t(y, t) - B\mathbf{F}(0, y, t) \ . \tag{17}$$

For a fourth-order accurate difference approximation we will need two extra numerical boundary conditions. Our principles for deriving these two conditions are as follows:

Principle 1: Apply the interior equation (12) on the boundary, $\nu = 0$.

Principle 2: Apply equation (17) to second-order accuracy on the boundary; thus we choose

$$\begin{aligned} B_{2h}\mathbf{v} &:= B_0\Big(A_1(D_+D_-)\mathbf{v}_0 + A_2\partial_y^2\mathbf{v}_0\Big) + B_1\Big(A_1 D_0(D_+D_-)\mathbf{v}_0 + A_2\partial_y^2 D_0\mathbf{v}_0\Big) \\ \mathbf{g}^{II} &:= \partial_t \mathbf{g}(y, t) - B\mathbf{F}(0, y, t) \ . \end{aligned}$$

Thus our discrete scheme is defined by

$$\begin{cases} \partial_t \mathbf{v}_\nu = A_1 \Delta_h \mathbf{v}_\nu + A_2 \partial_y^2 \mathbf{v}_\nu, & \nu = 0, 1, 2, \dots \ , \\ \mathbf{v}_\nu(y, 0) = 0, & \nu = -2, -1, 0, 1, 2, \dots \ , \\ B_0 \mathbf{v}_0(y, t) + B_1 D_h \mathbf{v}_0(y, t) = \mathbf{g}^I, & \\ B_{2h}\mathbf{v}_0 = \mathbf{g}^{II} \ . & \end{cases} \tag{18}$$

We now proceed, as in the continuous case, to determine an equivalent condition for stability. We Fourier and Laplace transform (18) with respect to y and t, respectively, and obtain

$$s\hat{\mathbf{v}}_\nu = A_1 \Delta_h \hat{\mathbf{v}}_\nu - \omega^2 A_2 \hat{\mathbf{v}}_\nu, \tag{19}$$
$$B_0 \hat{\mathbf{v}}_0 + B_1 D_h \hat{\mathbf{v}}_0 = \hat{\mathbf{g}}^I, \quad B_{2h}\hat{\mathbf{v}}_0 = \mathbf{g}^{II} \tag{20}$$

Corresponding to the continuous case, the general solution of (19) belonging to L_{2h} is of the form

$$\hat{\mathbf{v}}_\nu = \sum_{j=1}^{2n} \sigma_j \kappa_j^\nu \mathbf{g}_j. \tag{21}$$

where $|\kappa_j| < 1$ for $Re(s) > 0$. There will be n roots κ_j that approximate the continuous problem, for $h\sqrt{s + \omega^2} \ll 1$, along with n spurious roots. Substituting this expression into (20) gives us again a system of the form (9). Corresponding to Theorem 4 we have

Theorem 5 *The problem (18) is stable if, and only if, there are constants K_1 and α such that, for all ω and all s with* $\mathrm{Re}(s) > \alpha$, *a discrete estimate of type (10) holds.*

3.1 Stability of a scalar parabolic problem

We now consider the model problem of the heat equation in one-space dimension on the half line $x \geq 0$ for which we analyze the stability and accuracy in some detail. The function $u = u(x,t)$ satisfies

$$\begin{cases} u_t = u_{xx} + F & \text{for } x > 0 \\ b_0 u(0,t) + b_1 u_x(0,t) = g(t) & \\ u(x,0) = f(x) & \text{for } x \geq 0 \end{cases} . \tag{22}$$

We take the real constants b_0 and b_1 to have opposite sign and not both zero so that the problem is well-posed.

Using our principle we apply the equation on the boundary and we approximate equation (17) to second-order accuracy. Thus we have the following scheme:

$$\begin{cases} \frac{d}{dt} v_\nu = \Delta_h v_\nu + F(x_\nu, t) & \text{for } \nu = 0,1,2,3,\ldots \\ b_0 v_0 + D_h v_0 = g(t) & \\ b_0 (D_+ D_-) v_0 + b_1 (D_0 D_+ D_-) v_0 = g_t(t) - \{b_0 F(0,t) + b_1 F_x(0,t)\} & \\ v_\nu(0) = f(x_\nu) & \text{for } \nu = -2,-1,0,1,\ldots \end{cases} \tag{23}$$

The extra boundary condition has only been approximated to second-order; we will see that the overall accuracy is none-the-less fourth-order.

We first analyze the Dirichlet problem, $b_0 = 1$ and $b_1 = 0$. Note that in this case the scheme (23) is equivalent to the following method

$$\begin{cases} \frac{d}{dt} v_\nu = \Delta_h v_\nu + F(x_\nu, t) & \text{for } \nu = 0,1,2,3,\ldots \\ v_0 = g(t) - F(0,t) & \\ (D_+ D_-)^2 v_0 = 0 & \\ v_\nu(0) = f(x_\nu) & \text{for } \nu = -2,-1,0,1,2,3,\ldots \end{cases}$$

where the second numerical boundary condition has been replaced by an extrapolation condition, $(D_+D_-)^2 v_0 = (D_+)^4 v_{-2} = 0$.

By subtracting out a solution to the Cauchy problem we can assume that $F = f = 0$. An equation for the error $w_\nu(t) = u(x_\nu, t) - v_\nu(t)$ can be formed. The error equation is

$$\begin{cases} \frac{d}{dt} w_\nu = \Delta_h w_\nu & \text{for } \nu = 0,1,2,3,\ldots \\ w_0 = h^4 g_1(t) & \\ (D_+ D_-) w_0 = h^2 g_2(t) & \\ w_\nu(0) = 0 & \text{for } \nu = -2,-1,0,1,2,3,\ldots \end{cases} \tag{24}$$

Here g_1 and g_2 come from the truncation error and will be $O(1)$ for smooth solutions (although g_1 would normally be zero in the Dirichlet case we keep this more general form for later use). If we Laplace transform in time and look for a solution of the form $\hat{w}_\nu = \sigma \kappa^\nu$ then we obtain the characteristic equation

$$sh^2 = (\kappa - 2 + \kappa^{-1})\Big(1 - \frac{1}{12}(\kappa - 2 + \kappa^{-1})\Big) . \tag{25}$$

There are four roots to this equation, κ_j, $j = 1,2,3,4$. For $Re(s) > 0$ there are exactly two roots with $\kappa_j < 1$. Let κ_1 and κ_2 be the two (distinct) roots with $|\kappa_\nu| \leq 1$ (we treat the case $\kappa_1 = \kappa_2$ later). The general solution in L_{2h} is thus of the form

$$\hat{w}_\nu = \sigma_1 \kappa_1^\nu + \sigma_2 \kappa_2^\nu .$$

Applying the boundary conditions gives

$$\begin{aligned} \sigma_1 + \sigma_2 &= h^4 \hat{g}_1, \\ (\kappa_1 - 2 + \kappa_1^{-1})\sigma_1 + (\kappa_2 - 2 + \kappa_2^{-1})\sigma_2 &= h^4 \hat{g}_2, \end{aligned}$$

with solution

$$\sigma_1 = \frac{(\kappa_2 - 2 + \kappa_2^{-1})\hat{g}_1 - \hat{g}_2}{(\kappa_2 - \kappa_1)(1 - \frac{1}{\kappa_1 \kappa_2})} h^4 \quad , \quad \sigma_2 = \frac{\hat{g}_2 - (\kappa_1 - 2 + \kappa_1^{-1})\hat{g}_1}{(\kappa_2 - \kappa_1)(1 - \frac{1}{\kappa_1 \kappa_2})} h^4 .$$

Since $\kappa_1 \neq \kappa_2$, to show stability we need an estimate for $(1 - \frac{1}{\kappa_1 \kappa_2})^{-1}$. Since κ_1 and κ_2 both satisfy the characteristic equation it follows that

$$(\kappa_1 - 2 + \kappa_1^{-1})(1 - \frac{1}{12}(\kappa_1 - 2 + \kappa_1^{-1})) = (\kappa_2 - 2 + \kappa_2^{-1})(1 - \frac{1}{12}(\kappa_2 - 2 + \kappa_2^{-1}))$$

and thus

$$(\kappa_1-\kappa_2)(1-\frac{1}{\kappa_1\kappa_2})(12-(\kappa_1-2+\kappa_1^{-1})-(\kappa_2-2+\kappa_2^{-1}))=0 \quad .$$

Therefore κ_1 and κ_2 satisfy $\kappa_1-2+\kappa_1^{-1}+\kappa_2-2+\kappa_2^{-1}=12$ or $(\kappa_1+\kappa_2)(1+\frac{1}{\kappa_1\kappa_2})=16$. This implies (using $|\kappa_\nu|\le 1$) that

$$|1-\frac{1}{\kappa_1\kappa_2}|\ge 6 \ .$$

Thus the scheme is stable. For $|sh^2|\ll 1$, $\kappa_1\sim 1-\sqrt{s}h$ and $\kappa_2\sim 7-4\sqrt{(3)}\approx .0718$ and thus $\sigma_i=O(\hat{g}_i h^4)$. This proves that the scheme is fourth-order accurate. In the case $\kappa_1=\kappa_2$ there is a double root with $\kappa=4-\sqrt{15}$ and the analysis must be altered. In this situation the general solution is

$$\hat{v}_\nu=\sigma_1\kappa^\nu+\sigma_2\nu\kappa^\nu \ .$$

and the solution is

$$\sigma_1=\hat{g}_1 h^4 \quad , \quad \sigma_2=\frac{\hat{g}_2-(\kappa-2+\kappa^{-1})\hat{g}_1}{\kappa-\kappa^{-1}}h^4 \quad .$$

The required estimate follows. Thus we have shown that the scheme with Dirichlet boundary conditions is stable.

We now consider the case of Neumann boundary conditions, $b_1=1$ and $b_0=0$.

$$\begin{cases} \frac{d}{dt}v_\nu=\Delta_h v_\nu+F(x_\nu) & \text{for } \nu=0,1,2,3,\ldots \\ D_h v_0=g(t) & \\ D_0(D_+D_-)v_0=g_t(t)-F_x(0,t) & \\ v_\nu=f(x_\nu) & \text{for } \nu=-2,-1,0,1,2,3,\ldots \end{cases} \tag{26}$$

The analysis for this equation proceeds in the same way as the Dirichlet case. This can be seen by writing down the equations satisfied by $w_\nu=D_0v_\nu$ which are the same form as the equations in the Dirichlet case. Given w_ν, v_ν is determined up to a constant from $D_0v_\nu=w_\nu$. Note that the solution to (26) is also only determined up to a constant.

In the general situation $b_0\ne 0$ and $b_1\ne 0$ the equations defining σ_1 and σ_2 are

$$\begin{bmatrix} b_0+\frac{b_1}{h}\Delta_0\kappa_1(1-\frac{1}{6}\Delta\kappa_1) & b_0+\frac{b_1}{h}\Delta_0\kappa_2(1-\frac{1}{6}\Delta\kappa_2) \\ b_0\Delta\kappa_1+\frac{b_1}{h}\Delta_0\kappa_1\Delta\kappa_1 & b_0\Delta\kappa_2+\frac{b_1}{h}\Delta_0\kappa_2\Delta\kappa_2 \end{bmatrix}\begin{bmatrix}\sigma_1\\ \sigma_2\end{bmatrix}=\begin{bmatrix}h^4g_1\\ h^1g_2\end{bmatrix}$$

where

$$\Delta\kappa_i:=\kappa_i-2+\kappa_i^{-1} \ \text{ and } \ \Delta_0\kappa_i:=\frac{1}{2}(\kappa_i-\kappa_i^{-1}).$$

Let $\delta>0$ be a small parameter, independent of h, but sufficiently small, $0<h\ll\delta$. We consider the two cases of $|\sqrt{s}h|<\delta$ and $|\sqrt{s}h|\ge\delta$.

Case 1: $|\sqrt{s}h|<\delta$ In this case κ_1 and κ_2 are close to there values at $\sqrt{s}h=0$,

$$\kappa_1=1-\alpha\delta \quad \text{where } |\alpha|<1, \quad Re(\alpha)>0$$

and

$$\kappa_2=\mu_0+K\delta^2 \quad \text{where } \mu_0=7-\sqrt{48} \ .$$

Here K denotes a generic constant independent of δ and h. Under these conditions

$$\begin{aligned} \Delta\kappa_1 &= \alpha^2\delta^2+K\delta^3 \\ \Delta_0\kappa_1 &= -\alpha\delta+K\delta^2 \\ \Delta\kappa_2 &= (\mu_0+\mu_0^{-1}-2)+K\delta^2=12+K\delta^2 \\ \Delta_0\kappa_2 &= \frac{1}{2}(\mu_0-\mu_0^{-1})+K\delta^2:=C_2+K\delta^2 \quad , \quad C_2\approx -6.93 \end{aligned}$$

and thus the equations determining σ_1 and σ_2 are

$$\begin{bmatrix} b_0+\frac{b_1}{h}(-\alpha\delta+K\delta^2) & b_0+\frac{b_1}{h}(-C_2+K\delta^2) \\ hb_0(\alpha^2\delta^2+K\delta^3)+b_1(-\alpha^3\delta^3+K\delta^4) & hb_0(12+K\delta^2)+b_1(6C_2+K\delta^2) \end{bmatrix}\begin{bmatrix}\sigma_1\\ \sigma_2\end{bmatrix}=\begin{bmatrix}h^4g_1\\ h^5g_2\end{bmatrix} \ .$$

To leading order the above matrix is given by

$$\begin{bmatrix} b_0 + \frac{b_1}{h}(-\alpha\delta) & b_0 + \frac{b_1}{h}(-C_2) \\ 0 & b_1(6C_2) \end{bmatrix}$$

Since $Re(\alpha) > 0$ and $b_0 b_1 < 0$ it follows that we can obtain an estimate for σ_1 and σ_2. This shows that the scheme is stable for $\sqrt{s}h < \delta$. If $\delta = \mathcal{O}(h)$ then the scheme is also fourth-order accurate since $\sigma_1 = \mathcal{O}(h^4)$ and $\sigma_2 = \mathcal{O}(h^5)$.

Case 2: $\sqrt{s}h \geq \delta$ In this case both κ_1 and κ_2 are bounded away from 1,

$$|\kappa_1 - 1| \geq K\delta \quad , \quad |\kappa_2 - 1| \geq K\delta$$

and thus

$$|\Delta_0\kappa_1| \geq K\delta \quad , \quad |\Delta_0\kappa_2| \geq K\delta \ .$$

The system can be written in the form

$$\begin{bmatrix} hb_0(\Delta_0\kappa_1)^{-1} + \frac{b_1}{2}(1 - \frac{1}{6}\Delta\kappa_1) & hb_0(\Delta_0\kappa_2)^{-1} + \frac{b_1}{2}(1 - \frac{1}{6}\Delta\kappa_2) \\ hb_0\Delta\kappa_1(\Delta_0\kappa_1)^{-1} + \frac{b_1}{2}\Delta\kappa_1 & hb_0\Delta\kappa_2(\Delta_0\kappa_2)^{-1} + \frac{b_1}{2}\Delta\kappa_2 \end{bmatrix} \begin{bmatrix} \Delta_0\kappa_1\sigma_1 \\ \Delta_0\kappa_2\sigma_2 \end{bmatrix} = \begin{bmatrix} h^5 g_1 \\ h^5 g_2 \end{bmatrix}$$

To leading order this matrix is

$$A = \begin{bmatrix} \frac{b_1}{2}(1 - \frac{1}{6}\Delta\kappa_1) & \frac{b_1}{2}(1 - \frac{1}{6}\Delta\kappa_2) \\ \frac{b_1}{2}\Delta\kappa_1 & \frac{b_1}{2}\Delta\kappa_2 \end{bmatrix}$$

with

$$det(A) = \frac{b_1^2}{2}(\kappa_2 - \kappa_1)(1 - \frac{1}{\kappa_1\kappa_2}) \ .$$

The value of $det(A)$ can be estimated using the results from the case of Dirichlet boundary conditions and thus we can get an estimate for σ_1 and σ_2. This shows that the scheme is fourth-order accurate and stable in the case of mixed boundary conditions, $b_0 \neq 0$ and $b_1 \neq 0$.

3.2 A simplified approach to local stability

In the general case it may be difficult to determine analytically whether a particular scheme is stable. However, it is much easier, especially with the aid of a symbolic algebra package, to determine whether a scheme is locally stable and accurate. In our context a scheme is locally stable if it is stable for $h\sqrt{s+\omega^2} \ll 1$. In this limit the roots of the characteristic equation are well defined and can be divided into a set of roots that approximate the solution to the continuous problem and a set of roots that belong to the spurious part of the solution. We now return to the two-dimensional parabolic system and discuss how the question of local stability can be simplified to a question about the spurious solution. We also show why, in general, the extra numerical boundary condition (17), need only be applied to second-order accuracy. Thus we consider (19)-(20) for $h\sqrt{s+\omega^2} \ll 1$. The general solution of (19) belonging to L_{2h} is of the form

$$\hat{\mathbf{v}}(x_\nu) \simeq \hat{\mathbf{u}}(x_\nu) + \hat{\mathbf{v}}_S(x_\nu).$$

Here $\hat{\mathbf{u}}(x_\nu)$ represents the general solution of the continuous problem and

$$\hat{\mathbf{v}}_S(x_\nu) = \sum_{j=n}^{2n} \sigma_j \kappa_j^\nu \mathbf{w}_j$$

is the so called spurious part of the solution. The eigenvalue κ_j and eigenfunction $\mathbf{w}_j$ are the solutions of

$$(sh^2 + A_2\omega^2h^2)\mathbf{w} = A_1\Big(\frac{(\kappa-1)^2}{\kappa} - \frac{1}{12}\frac{(\kappa-1)^4}{\kappa^2}\Big)\mathbf{w}.$$

The spurious eigenvalues satisfy $\kappa_j \sim 7 - 4\sqrt{3} \approx .072$ as $h \to 0$. We introduce this representation into the boundary conditions and obtain

$$B_0\hat{\mathbf{u}} + B_1D_h\hat{\mathbf{u}} + B_0\hat{\mathbf{v}}_S + B_1D_h\hat{\mathbf{v}}_S = \hat{\mathbf{g}}^I, \tag{27}$$

$$B_{2h}\hat{\mathbf{u}} + B_{2h}\hat{\mathbf{v}}_S = \hat{\mathbf{g}}^{II}. \tag{28}$$

For simplicity we assume that both B_0 and B_1 are diagonal so that the boundary conditions decouple and are either of Dirichlet type or of mixed type. Let $\boldsymbol{\sigma}^{I} = (\sigma_1, \dots, \sigma_n)^T$, $\boldsymbol{\sigma}^{II} = (\sigma_{n+1}, \dots, \sigma_{2n})^T$, denote the coefficients of $\hat{\mathbf{u}}, \hat{\mathbf{v}}_S$, respectively. We regard the numerical boundary condition (28) as a system of equations for $\boldsymbol{\sigma}^{II}$. We assume that it is nonsingular. Since $\hat{\mathbf{u}}$ corresponds to the accurate part of the solution it follows that $B_{2h}\hat{\mathbf{u}} = \mathcal{O}(1)$. However, since the κ's come from the spurious part of the solution we expect that $B_{2h}\kappa^\nu = \mathcal{O}(h^{-p})\kappa^\nu$ where $p = 2$ if the boundary conditions are Dirichlet and $p = 3$ if the boundary conditions are mixed. This comes from the fact that $(D_+D_-)\kappa^\nu = \mathcal{O}(h^{-2})\kappa^\nu$ and $D_0(D_+D_-)\kappa^\nu = \mathcal{O}(h^{-3})\kappa^\nu$. With these assumptions

$$|\boldsymbol{\sigma}^{II}| \le \text{ const. } (h^p|g^{II}| + h^p|\boldsymbol{\sigma}^{I}|).$$

Introducing this expression into the true boundary conditions (27) gives us a perturbation of (9), that is,

$$(\mathcal{B} + \mathcal{O}(h^4))\boldsymbol{\sigma}^{I} = \hat{\mathbf{g}}^I + \mathcal{O}(h^{2-p}|\boldsymbol{\sigma}^{II}|) = \hat{\mathbf{g}}^I + \mathcal{O}(h^2\hat{\mathbf{g}}^I + h^2|\boldsymbol{\sigma}^{I}|) \tag{29}$$

If the continuous problem is well-posed, then (29) is nonsingular and

$$|\boldsymbol{\sigma}^{I}| \le \text{ const. } |\hat{\mathbf{g}}^I| + \mathcal{O}(h^2|\hat{\mathbf{g}}^{II}|).$$

Therefore, the solution of (19)-(20) is uniquely determined and we obtain the estimate

$$\|\mathbf{u}\|_h^2 + \|D_h\mathbf{u}\|_h^2 \le \text{ const. } \left(|\mathbf{g}^I|^2 + h^4|\mathbf{g}^{II}|^2\right). \tag{30}$$

Thus we have shown that if the the continuous problem is well-posed and if the spurious solution is uniquely determined by the extra boundary condition, then the approximation is locally stable (that is for $\sqrt{s+\omega^2}h \ll 1$).

For accuracy we consider the error equation in which case $\hat{\mathbf{g}}^I = \mathcal{O}(h^4)$ and $\hat{\mathbf{g}}^{II} = \mathcal{O}(h^2)$ (because the extra numerical boundary condition is only approximated to second order). From the estimate (30), however, we see that the overall accuracy is still fourth-order.

Remark. The local stability and the accuracy can, in most cases, be determined. However, the global stability can be difficult to verify analytically. Numerically, however, a scheme that is locally stable but not globally stable will be easy to see since the numerical solution will have high-frequency components in space and/or time since they will occur for $h\sqrt{s+\omega^2} = \mathcal{O}(1)$. Thus one can be fairly confident that if a locally stable scheme behaves itself numerically, even for short times, then it is stable in the global sense as well.

4 The Incompressible Navier-Stokes Equations

In this section we consider the initial boundary value problem for the incompressible Navier-Stokes equations,

$$\left\{\begin{array}{rcll} \mathbf{u}_t + (\mathbf{u}\cdot\nabla)\mathbf{u} + \nabla p &=& \nu\Delta\mathbf{u} + \mathbf{F} & \text{for } x \in \Omega \\ \nabla\cdot\mathbf{u} &=& 0 & \text{for } x \in \Omega \\ B(\mathbf{u}, p) &=& 0 & \text{for } x \in \partial\Omega \\ \mathbf{u}(\mathbf{x}, 0) &=& \mathbf{f}(\mathbf{x}) & \text{at } t = 0 \end{array}\right. \tag{31}$$

We require the initial conditions to be divergence free, $\nabla\cdot\mathbf{f} = 0$. There are n boundary conditions $B(\mathbf{u}, p) = 0$, where n is equal to the number of space dimensions. For example, on a stationary no-slip wall the boundary condition is $\mathbf{u} = \mathbf{0}$. For numerical reasons it is easier to solve a different set of equations replacing the condition $\nabla\cdot\mathbf{u} = 0$ by an equation for the pressure:

$$\left\{\begin{array}{rcll} \mathbf{u}_t + (\mathbf{u}\cdot\nabla)\mathbf{u} + \nabla p &=& \nu\Delta\mathbf{u} + \mathbf{F} & \text{for } x \in \Omega \\ \Delta p - (\nabla u\cdot\mathbf{u}_x + \nabla v\cdot\mathbf{u}_y + \nabla w\cdot\mathbf{u}_z) - \nabla\cdot\mathbf{F} &=& 0 & \text{for } x \in \Omega \\ B(\mathbf{u}, p) &=& 0 & \text{for } x \in \partial\Omega \\ \nabla\cdot\mathbf{u} &=& 0 & \text{for } x \in \partial\Omega \\ \mathbf{u}(\mathbf{x}, 0) &=& \mathbf{f}(\mathbf{x}) & \text{at } t = 0 \end{array}\right. \tag{32}$$

In addition to the standard boundary conditions $B(\mathbf{u}, p) = 0$ the boundary condition $\nabla\cdot\mathbf{u} = 0$ is added. This latter condition is an essential boundary condition for this formulation and ensures that (32) is equivalent to the original formulation (31). There has been much discussion in the literature as to the proper boundary condition for the pressure equation, see for example [2]. From this simple argument we see that the correct boundary condition for the pressure is $\nabla\cdot\mathbf{u} = 0$. For further discussion of this point see [3].

We now proceed, by mode analysis, to consider the well-posedness of of (31), or rather a simplified version of this problem for the Stokes equations. It is well known that (31) is well-posed, see for example Ladyzhenskaya [5]. However, it is instructive to present the the mode analysis of the continuous problem since it resembles the stability analysis of the discretized problem.

After dropping the lower-order terms and setting the kinematic-viscosity $\nu = 1$ we are led to consider the following model problem for the Stokes equations on the half space $H = \{(x, y, t) : x \geq 0, \;\; -\infty < y < +\infty, \;\; t \geq 0\}$

$$\left\{ \begin{array}{rl} u_t + p_x - (u_{xx} + u_{yy}) - F_1 = 0 & \text{for} \quad \mathbf{x} \in H \\ v_t + p_y - (v_{xx} + v_{yy}) - F_2 = 0 & \text{for} \quad \mathbf{x} \in H \\ u_x + v_y = 0 & \text{for} \quad \mathbf{x} \in H \\ (u, v) = (g_1(y,t), g_2(y,t)) \quad , \quad u_x + v_y = 0 & \text{for} \quad x = 0 \\ (u(x,y,0), v(x,y,0) = (f_1(x,y), f_2(x,y)) \quad , \quad \nabla \cdot (u_0, v_0) = 0 & \text{at} \quad t = 0 \end{array} \right. \tag{33}$$

To be definite we have chosen Dirichlet boundary conditions for u and v. By subtracting out functions that satisfy the forced equations and the initial conditions (but not the boundary conditions) one may assume that $(F_1, F_2) = \mathbf{0}$ and $(f_1, f_2) = \mathbf{0}$. We look for solutions in L_2 that are 2π periodic in y. The functions $g_1(y,t)$ and $g_2(y,t)$ are thus assumed to be periodic in y. By taking the divergence of the momentum equation it follows that the divergence satisfies the equation

$$(u_x + v_y)_t = \Delta(u_x + v_y) - \Delta p \; .$$

where $\Delta = \partial^2/\partial x^2 + \partial^2/\partial y^2$. Observing the boundary condition $u_x + v_y = 0$, it follows that the divergence remains identically zero if and only if

$$\begin{array}{rl} u_x + v_y = 0 & \text{at } t = 0, \\ \Delta p = 0 & \text{for all times.} \end{array}$$

Thus we have essentially shown the equivalence of systems (31) and (32).

Remark: In numerical computations one often replaces $\Delta p = 0$ by

$$\Delta p = \alpha(u_x + v_y) \tag{34}$$

in which case

$$(u_x + v_y)_t = \Delta(u_x + v_y) - \alpha(u_x + v_y) \; .$$

This term acts as a damping on the divergence provided $\alpha > 0$. This damping may be helpful if $u_x + v_y$ is not zero due to errors in the initial conditions or truncation errors.

The analysis proceeds by first Fourier transforming the equations in y and Laplace transforming in t. Let $\hat{u}(x, \omega, s)$ denote the transformed velocity. Then

$$\begin{array}{r} s\hat{u} + \hat{p}_x - (\hat{u}_{xx} - \omega^2 \hat{u}) = 0 \\ s\hat{v} + i\omega\hat{p} - (\hat{v}_{xx} - \omega^2 \hat{v}) = 0 \\ \hat{p}_{xx} - \omega^2 \hat{p} = 0 \\ \hat{u}(0, \omega, s) = g_1(\omega, s) \quad , \quad \hat{v}(0, \omega, s) = g_2(\omega, s) \end{array} \quad , \quad \hat{u}_x(0, \omega, s) + i\omega\hat{v}(0, \omega, s) = 0$$

The general solution in L_2 is given by

$$\left\{ \begin{array}{rcl} \hat{p}(x, \omega, s) & = & P(\omega, s) e^{-|\omega| x} \\ \hat{u}(x, \omega, s) & = & U(\omega, s) e^{-\sqrt{s+\omega^2} x} + \frac{|\omega| P(\omega, s)}{s} (e^{-|\omega| x} - e^{-\sqrt{s+\omega^2} x}) \\ \hat{v}(x, \omega, s) & = & V(\omega, s) e^{-\sqrt{s+\omega^2} x} - \frac{i\omega P(\omega, s)}{s} (e^{-|\omega| x} - e^{-\sqrt{s+\omega^2} x}) \end{array} \right. \; . \tag{35}$$

The free coefficients U, V, and P are determined by the boundary conditions,

$$\begin{array}{rcl} U(\omega, s) & = & g_1(\omega, s) \\ V(\omega, s) & = & g_2(\omega, s) \\ \frac{|\omega| P(\omega, s)}{s} (\sqrt{s + \omega^2} - |w|) & = & \sqrt{s + \omega^2} g_1(\omega, s) - i\omega g_2(\omega, s). \end{array}$$

We can solve for P provided $Re(s) \geq 0$, $s \neq 0$ and $\omega \neq 0$. When $\omega = 0$ we are free to choose $P(0, s)$ since the mean value of the pressure does not change the solution for (u, v). Given a value for $P(0, s)$ we can invert the transformation and obtain a unique solution.

Remark: Note that

$$\begin{aligned} \lim_{s\to 0} \frac{|w|}{s}(\sqrt{s+\omega^2}-\omega) &= \frac{1}{2} \\ \lim_{s\to 0} \frac{|w|}{s}(e^{-|w|x)} - e^{-\sqrt{s+\omega^2}x}) &= \frac{1}{2}xe^{-|w|x} \end{aligned}$$

and therefore the solution to (35) is also well defined at $s = 0$.

5 Discrete boundary conditions for the Incompressible Navier-Stokes Equations

We now apply our principle to derive numerical boundary conditions for a fourth-order accurate difference approximation to the incompressible Navier-Stokes equations. From the point of view of stability we may drop the lower order terms in the equations. Thus we are led to study the Stokes equations. The velocity-pressure formulation for these equations in two-space dimensions on the half plane $x \geq 0$ is

$$\left\{ \begin{aligned} u_t + p_x &= u_{xx} + u_{yy} && \text{for } x > 0 \\ v_t + p_y &= v_{xx} + v_{yy} && \text{for } x > 0 \\ p_{xx} + p_{yy} &= 0 && \text{for } x > 0 \\ (u(0,y,t), v(0,y,t)) &= (g_u(y,t), g_v(y,t)) && \\ u_x(0,y,t) + v_y(0,y,t) &= 0 && \end{aligned} \right. \tag{36}$$

The extra boundary condition $u_x + v_y = 0$ is required to ensure that this system is equivalent to the original velocity-divergence formulation. We look for solutions that are 2π periodic in y.

We discretize to fourth-order in the x-direction, keeping y and t continuous. Letting $U_\nu(y,t)$, $V_\nu(y,t)$ and $P_\nu(y,t)$ be the discrete approximation, the semi-discrete system is

$$\left\{ \begin{aligned} \tfrac{d}{dt}U_\nu + D_h P_\nu &= \Delta_h U_\nu + \partial_{yy} U_\nu && \text{for } \nu = 0,1,2... \\ \tfrac{d}{dt}V_\nu + \partial_y P_\nu &= \Delta_h V_\nu + \partial_{yy} V_\nu && \text{for } \nu = 0,1,2... \\ \Delta_h P_\nu + \partial_{yy} P_\nu &= 0 && \text{for } \nu = 0,1,2... \\ (U_0, V_0) &= (g_u(y,t), g_v(y,t)) && \\ D_h U_0 + \partial_y V_0 &= 0. && \end{aligned} \right. \tag{37}$$

The system (36) is an incomplete parabolic system since there is no time dependence in the pressure equation. However, we still use our principles to guide us in deriving appropriate boundary conditions. We must then check the accuracy and stability of the resulting scheme. In accordance with our first principle we have applied the interior equations on the boundary. Three extra numerical boundary conditions are required to determine the solution at two lines of fictitious points.

The divergence boundary condition $u_x + v_y = 0$ is a condition on u_x, since v and thus v_y is given on the boundary. This boundary condition on u_x takes priority over the Dirichlet boundary condition on u. Thus we form a numerical boundary condition from the x derivative of the u momentum equation:

$$(u_x)_t + p_{xx} = u_{xxx} + u_{xyy} \ .$$

This equation, which can be rewritten as $u_{xxx} + p_{yy} = -(v_y)_t + v_{yyy}$, is discretized to second-order accuracy on the boundary:

$$(D_0 D_+ D_-)U_0 + \partial_y^2 P_0 = -\partial_y \partial_t g_v + (\partial_y)^3 g_v \ := g_2 \ . \tag{38}$$

The Dirichlet boundary condition for v suggests that we apply the v momentum equation on the boundary to second order:

$$(D_+ D_-)V_0 - \partial_y P_0 = \partial_t g_v := g_3 \ . \tag{39}$$

The pressure equation is a not a parabolic equation and so does not fit with our analysis. Motivated by the desire to keep the pressure boundary conditions, as much as possible, independent of the velocity we choose

$$(D_+ D_-)P_0 + \partial_y^2 P_0 = 0 \ . \tag{40}$$

We now show that these numerical boundary conditions are appropriate.

Lemma 1 *The solution to (37)-(40) is locally stable and fourth-order accurate.*

A locally stable scheme is one that is stable for $\sqrt{s+\omega^2}h \ll 1$. It is easier to show local stability since the roots of the characteristic equation can be approximated for small $\sqrt{s+\omega^2}h$.

To analyze the stability and accuracy we Laplace transform in time and Fourier transform in y. Let $\hat{U}_\nu(\omega,s)$, $\hat{V}_\nu(\omega,s)$ and $\hat{P}_\nu(\omega,s)$ denote the transformed variables. The equation for the error is

$$\left\{\begin{array}{rcll} s\hat{U}_\nu + D_h\hat{P}_\nu &=& \Delta_h\hat{U}_\nu - \omega^2\hat{U}_\nu & \text{for } \nu=0,1,2... \\ s\hat{V}_\nu + i\omega\hat{P} &=& \Delta_h\hat{V}_\nu - \omega^2\hat{V}_\nu & \text{for } \nu=0,1,2... \\ \Delta_h\hat{P}_\nu - \omega^2\hat{P}_\nu &=& 0 & \text{for } \nu=0,1,2... \\ (\hat{U}_0,\hat{V}_0) &=& (0,0) & \\ D_h\hat{U}_0 &=& h^4 g_1 & \\ (D_0D_+D_-)\hat{U}_0 - \omega^2\hat{P}_0 &=& h^2 g_2 & \\ (D_+D_-)\hat{V}_0 - i\omega\hat{P}_0 &=& h^2 g_3 & \\ (D_+D_-)\hat{P}_0 - \omega^2\hat{P}_0 &=& h^2 g_4 & \end{array}\right. \tag{41}$$

A solution to these equations, satisfying $(\hat{U}_0,\hat{V}_0)=(0,0)$, can be written in the form

$$\left\{\begin{array}{rcl} \hat{U}_\nu &=& u_1[\kappa_1^\nu - \kappa_2^\nu] - \frac{1}{hs}q(\tau_1)p_1[\tau_1^\nu - \kappa_1^\nu] - \frac{1}{hs}q(\tau_2)p_2[\tau_2^\nu - \kappa_2^\nu] \\ \hat{V}_\nu &=& v_1[\kappa_1^\nu - \kappa_2^\nu] - \frac{i\omega}{s}p_1[\tau_1^\nu - \kappa_1^\nu] - \frac{i\omega}{s}p_2[\tau_2^\nu - \kappa_2^\nu] \\ \hat{P}_\nu &=& p_1\tau_1^\nu + p_2\tau_2^\nu \end{array}\right. \tag{42}$$

where τ_1, τ_2, κ_1 and κ_2 are roots of

$$\begin{array}{rcl} (\kappa-2+\kappa^{-1})\Big(1-\frac{1}{12}(\kappa-2+\kappa^{-1})\Big) &=& h^2(s+\omega^2) \\ (\tau-2+\tau^{-1})\Big(1-\frac{1}{12}(\tau-2+\tau^{-1})\Big) &=& h^2\omega^2 \end{array}$$

with $|\kappa_i|<1$, $|\tau_i|<1$, $i=1,2$ for $Re(s)>0$. For $|(s+\omega^2)|h^2 \ll 1$

$$\begin{array}{rcl} \kappa_1 &=& 1-\sqrt{s+\omega^2}h + \frac{1}{2}(s+\omega^2)h^2 + \mathcal{O}((s+\omega^2)^{3/2}h^3) \\ \kappa_2 &=& 7-4\sqrt{3} + \mathcal{O}((s+\omega^2)h^2) \\ \tau_1 &=& 1-|\omega|h + \frac{1}{2}|w|^2h^2 + \mathcal{O}(\omega^3h^3) \\ \tau_2 &=& 7-4\sqrt{3} + \mathcal{O}(\omega^2h^2) \end{array}$$

Note that $\kappa_1 \sim e^{-\sqrt{s+\omega^2}h} + \mathcal{O}(h^4)$, $\tau_1 \sim e^{-|\omega|h} + \mathcal{O}(h^4)$, and $\kappa_2 \sim \tau_2 \sim 7-4\sqrt{3} \approx .0718$. Define

$$\begin{array}{rcl} \mathcal{D}\kappa &:=& \frac{(\kappa-\kappa^{-1})}{2}\Big(1-\frac{1}{6}(\kappa-2+\kappa^{-1})\Big) \\ \Delta\kappa &:=& \kappa-2+\kappa^{-1} \\ \Delta_0\kappa &:=& \frac{1}{2}(\kappa-\kappa^{-1})\ . \end{array}$$

Substituting the equations (42) into the divergence boundary condition and the numerical boundary conditions (38)-(40) gives

$$u_1[\mathcal{D}\kappa_1 - \mathcal{D}\kappa_2] - p_1\frac{\mathcal{D}\tau_1}{hs}[\mathcal{D}\tau_1 - \mathcal{D}\kappa_1] - p_2\frac{\mathcal{D}\tau_2}{hs}[\mathcal{D}\tau_2 - \mathcal{D}\kappa_2] = h^5 g_1 \tag{43}$$

$$u_1[\Delta_0\kappa_1 - \Delta_0\kappa_2] - p_1\frac{\mathcal{D}\tau_1}{hs}[\Delta_0\tau_1 - \Delta_0\kappa_1] - p_2\frac{\mathcal{D}\tau_2}{hs}[\Delta_0\tau_2 - \Delta_0\kappa_2] - \frac{h^3\omega^2}{6}(p_1+p_2) = h^5 g_1 + \frac{h^5}{6}g_2 \tag{44}$$

$$v_1[\Delta\kappa_1 - \Delta\kappa_2] + p_1[-i\omega h^2 - \frac{i\omega}{s}(\Delta\tau_1 - \Delta\kappa_1)] + p_2[-i\omega h^2 - \frac{i\omega}{s}(\Delta\tau_2 - \Delta\kappa_2)] = h^4 g_3 \tag{45}$$

$$p_1[\Delta\tau_1 - \omega^2h^2] + p_2[\Delta\tau_2 - \omega^2h^2] = h^4 g_4 \tag{46}$$

Equation (44) is formed by combining (38) with the divergence boundary condition. Equations (43),(44),(46) will determine u_1, p_1, p_2. After solving for u_1, p_1, p_2 the remaining unknown, v_1 is obtained from (45). In matrix form the equations for u_1, p_1, p_2 are

$$A\begin{bmatrix} u_1 \\ p_1 \\ p_2 \end{bmatrix} = \begin{bmatrix} h^5 g_1 \\ h^5 \hat{g}_2 \\ h^4 g_4 \end{bmatrix}$$

where

$$A = \begin{bmatrix} [\mathcal{D}\kappa_1 - \mathcal{D}\kappa_2] & -\frac{\mathcal{D}\tau_1}{hs}[\mathcal{D}\tau_1 - \mathcal{D}\kappa_1] & -\frac{\mathcal{D}\tau_2}{hs}[\mathcal{D}\tau_2 - \mathcal{D}\kappa_2] \\ \Delta_0\kappa_1 - \Delta_0\kappa_2 & -\frac{\mathcal{D}\tau_1}{hs}[\Delta_0\tau_1 - \Delta_0\kappa_1] - \frac{h^3\omega^2}{6} & -\frac{\mathcal{D}\tau_2}{hs}[\Delta_0\tau_2 - \Delta_0\kappa_2] - \frac{h^3\omega^2}{6} \\ 0 & \Delta\tau_1 - \omega^2 h^2 & \Delta\tau_2 - \omega^2 h^2 \end{bmatrix} .$$

For $h\sqrt{s+\omega^2} \ll 1$ the solution to these equations is

$$\begin{aligned} u_1 &= \frac{1}{32\sqrt{3}}(-4g_1 + 4\hat{g}_2 - 5g_4)h^5 + \mathcal{O}((\sqrt{s+\omega^2}h)^5) \\ v_1 &= -\frac{1}{144}g_3 h^4 + \mathcal{O}((\sqrt{s+\omega^2}h)^5) \\ p_1 &= \frac{1}{6}(3g_1 + 3\hat{g}_2 + 2g_4)\frac{(|\omega| - \sqrt{s+\omega^2})}{|\omega|}h^4 + \mathcal{O}((\sqrt{s+\omega^2}h)^4) \\ p_2 &= \frac{1}{12}g_4 h^4 + \mathcal{O}((\sqrt{s+\omega^2}h)^5) \end{aligned}$$

and thus the scheme is locally stable and fourth-order accurate.

5.1 Alternative boundary conditions

For historical reasons we present a second set of numerical boundary conditions. These conditions are the ones that are used in the numerical results presented in the final section. They were devised before we had fully developed our principle for choosing numerical boundary conditions, although they follow a similar idea.

The conditions we use are to approximate the x-derivative of the divergence equation

$$(u_x + v_y)_x = u_{xx} + v_{xy} = 0$$

(instead of the x derivative of the u momentum equation). This equation is approximated to fourth-order accuracy,

$$\Delta_h \hat{U}_0 + i\omega D_h \hat{V}_0 = 0 . \tag{47}$$

We also apply the equations on the boundary although they are approximated to higher than second-order accuracy. (Using second-order accuracy here does not result in a fourth-order scheme). The equation to fourth-order is given on the boundary and the values for v and p at the second fictitious point are extrapolated as follows:

$$(D+)^6 \hat{V}_{-2} = 0 \tag{48}$$

$$(D+)^5 \hat{P}_{-2} = 0 . \tag{49}$$

This is like approximating the equation on the boundary with a one-sided difference scheme.

Thus we replace boundary conditions (38)-(40) by the boundary conditions (47)-(49).

We can analyze this scheme to show that it is locally stable. The unknown coefficients in the solution for the error are determined from

$$\begin{aligned} D_h \hat{U}_0 &= h^4 g_1 \\ \Delta_h \hat{U}_0 + i\omega D_h \hat{V}_0 &= h^4 g_2 \\ (D+)^6 \hat{V}_{-2} &= g_3 \\ (D+)^5 \hat{P}_{-2} &= g_4 . \end{aligned}$$

Following the argument presented previously leads to

$$\begin{aligned} u_1 &= \Big\{ -\frac{1}{4\sqrt{3}}g_1 + (\frac{\omega - \sqrt{s+\omega^2}}{s})(\frac{g_2}{4\sqrt{3}} + \frac{(2+\sqrt{3})g_3}{2^5 3^2\sqrt{3}})\Big\}h^5 + \mathcal{O}((\sqrt{s+\omega^2}h)^5) \\ v_1 &= -\frac{(7+4\sqrt{3})}{2^6 3^3}g_3 h^6 + \mathcal{O}((\sqrt{s+\omega^2}h)^7) \\ p_1 &= \big(-g_2 - \frac{(2+\sqrt{3})}{2^3 3^2}g_3\big)\frac{1}{\omega}h^4 + \mathcal{O}((\sqrt{s+\omega^2}h)^5) \\ p_2 &= -\frac{(3+2\sqrt{3})}{2^5 3^3}g_4 h^5 + \mathcal{O}((\sqrt{s+\omega^2}h)^6) \end{aligned}$$

Thus this scheme is fourth-order accurate and locally stable.

6 Numerical results for the Incompressible Navier-Stokes Equations

In this section we present some results from a computer program that has been written to solve the incompressible Navier-Stokes equations in complicated geometries in two and three-space dimensions. The grid construction program CMPGRD [1] is used to generate an overlapping grid for the region of interest. We solve the system of equations (32), discretized to fourth-order accuracy, together with the numerical boundary conditions (47)-(49). We also add a damping term to the pressure equation (cf. equation (34)). The solution is advanced in time by a method of lines approach. The velocity is advanced explicitly (with a Runge-Kutta method, for example) and at each stage in the time step the pressure is computed from the elliptic equation for the pressure. The pressure equation is solved either with sparse direct solvers, sparse iterative solvers (such as bi-conjugate gradient squared) or the multigrid algorithm. Details on the discretization and solution procedure, as well as more extensive convergence studies can be found in [3]. Readers interested in obtaining a copy of the programs should make enquiries to the first author (whensha@watson.ibm.com).

To illustrate the fourth-order accuracy of the method we present some convergence studies. We force the equations so that the true solution is known. In two space dimensions the equations are forced so that the exact solution will be

$$\begin{aligned} \mathbf{u}_{\text{true}}(x,y,t) &= \Big(\sin^2(fx)\sin(2fy)\cos(2\pi t) \;,\; -\sin(2fx)\sin^2(fy)\cos(2\pi t) \Big) \;, \\ p_{\text{true}}(x,y,t) &= \sin(fx)\sin(fy)\cos(2\pi t) \;. \end{aligned}$$

In table 1 we give results for the flow in a unit square with walls for boundaries. Indicated are the maximum errors in $\mathbf{u}$, p and $\nabla\cdot\mathbf{u}$. The divergence is calculated as $\nabla_4\cdot\mathbf{U}_i$ at all interior and boundary points. The estimated convergence rate σ, error $\propto h^\sigma$, is also shown. σ is estimated by a least squares fit to the maximum errors given in the table.

Grid	Error in $\mathbf{u}$	Error in p	Maximum in $\nabla\cdot\mathbf{u}$
20×20	1.2×10^{-3}	4.1×10^{-3}	1.2×10^{-2}
30×30	2.5×10^{-4}	6.8×10^{-4}	1.2×10^{-3}
40×40	7.9×10^{-5}	2.1×10^{-4}	2.4×10^{-4}
σ	3.9	4.0	5.6

Table 1: Errors for flow in a square at $t=1.$, and estimated convergence rate, $e\propto h^\sigma$, ($f=1$, $\nu=.05$)

In table 2 we give results for the flow in a unit circle. The solution and grid are shown in figure 1.

Grid	Error in $\mathbf{u}$	Error in p	Maximum in $\nabla\cdot\mathbf{u}$
$35\times 35\cup 55\times 11$	3.1×10^{-3}	1.0×10^{-2}	1.7×10^{-2}
$69\times 69\cup 109\times 21$	1.9×10^{-4}	6.4×10^{-4}	8.8×10^{-4}
σ	4.0	4.0	4.3

Table 2: Errors for flow in a circle at $t=1.$, and estimated convergence rate, $e\propto h^\sigma$, ($f=\frac{1}{2}$, $\nu=.05$)

As an example in three dimensions we show results for the flow between two spheres. In three-space dimensions the equations are forced so that the true solution is known and equal to

$$\begin{aligned} \mathbf{u}_{\text{true}}(x,y,z,t) &= \Big(\sin(fx)\cos(fy)\cos(fz)\cos(2\pi t) \;, \\ &\qquad \cos(fx)\sin(fy)\cos(fz)\cos(2\pi t) \;, \\ &\qquad -2\cos(fx)\cos(fy)\sin(fz)\cos(2\pi t) \Big) \;, \\ p_{\text{true}}(x,y,z,t) &= \sin(fx)\sin(fy)\sin(fz)\cos(2\pi t) \;. \end{aligned}$$

The spherical shell is the domain outside a sphere of radius $R_0 = \frac{1}{2}$ and inside a a concentric sphere of radius $R_1 = 1$. The grid for this region was created using two component grids; one component grid covers the top half of the domain and the second grid covers the bottom half. In table 3 results are shown for computations in this spherical shell.

Grid	Error in $\mathbf{u}$	Error in p	Maximum in $\nabla \cdot \mathbf{u}$
$25^2 \times 7 \cup 25^2 \times 7$	1.1×10^{-3}	3.8×10^{-3}	2.6×10^{-3}
$37^2 \times 10 \cup 37^2 \times 10$	2.2×10^{-4}	7.0×10^{-4}	4.8×10^{-4}
$49^2 \times 13 \cup 49^2 \times 13$	7.3×10^{-5}	2.2×10^{-4}	1.7×10^{-4}
σ	4.0	4.2	4.2

Table 3: Errors for flow in a spherical shell at $t = .5$, and estimated convergence rate, $e \propto h^\sigma$, ($f = \frac{1}{4}$, $\nu = .05$)

As a final example results are shown from the computation of the two-dimensional flow past a cylinder. The cylinder is located at the origin and has radius $\frac{1}{2}$. The computational domain is $[x_a, x_b] \times [y_a, y_b] = [-2.5, 15] \times [-3.5, 3.5]$. The kinematic viscosity is $\frac{1}{100}$. The top and bottom boundaries are slip walls ($\mathbf{n} \cdot \mathbf{u} = 0$,$\partial_n(\mathbf{t} \cdot \mathbf{u}) = 0$). Here $\mathbf{n}$ is the inward facing unit normal vector and $\mathbf{t}$ is the unit tangent vector. The left boundary is inflow ($\mathbf{n} \cdot \mathbf{u} = 1$, $\mathbf{t} \cdot \mathbf{u} = 0$), and the right boundary outflow ($\partial_n p = -2\nu/(\frac{1}{2}(y_b - y_a))^2$, $\partial_n^2(\mathbf{n} \cdot \mathbf{u}) = 0$, $\partial_n^2(\mathbf{t} \cdot \mathbf{u}) = 0$). The cylinder has no-slip boundary conditions ($\mathbf{u} = 0$). The Reynolds number based on the cylinder diameter and a velocity of 1 is $R_e = 100$. At this Reynolds number the steady symmetric solution is unstable and an unsteady flow develops. The unsteady flow takes a long time to develop – it is not until time $t = 40$ that the Kármán vortex street is clearly visible. See figures (2-4). The ratio of the maximum divergence to the maximum vorticity was always less than about 3×10^{-3}.

References

[1] G. Chesshire and W. Henshaw, *Composite overlapping meshes for the solution of partial differential equations*, J. Comp. Phys., 90 (1990), pp. 1–64.

[2] P. M. Gresho and R. L. Sani, *On the pressure boundary conditions for the incompressible Navier-Stokes equations*, International Journal for Numerical Methods in Fluids, 7 (1987), pp. 1111–1145.

[3] W. Henshaw, *A fourth-order accurate method for the incompressible Navier-Stokes equations on overlapping grids*, J. Comp. Phys., 113 (1994), pp. 13–25.

[4] H.-O. Kreiss and J. Lorenz, *Initial-Boundary Value Problems and the Navier-Stokes Equations*, Academic Press, 1989.

[5] O. A. Ladyzhenskaya, *The Mathematical Theory of Viscous Incompressible Flow*, Gordon and Breach, New York, 1963.

[6] J. Strikwerda, *Finite Difference Schemes and Partial Differential Equations*, Wadsworth and Brooks/Cole, 1989.

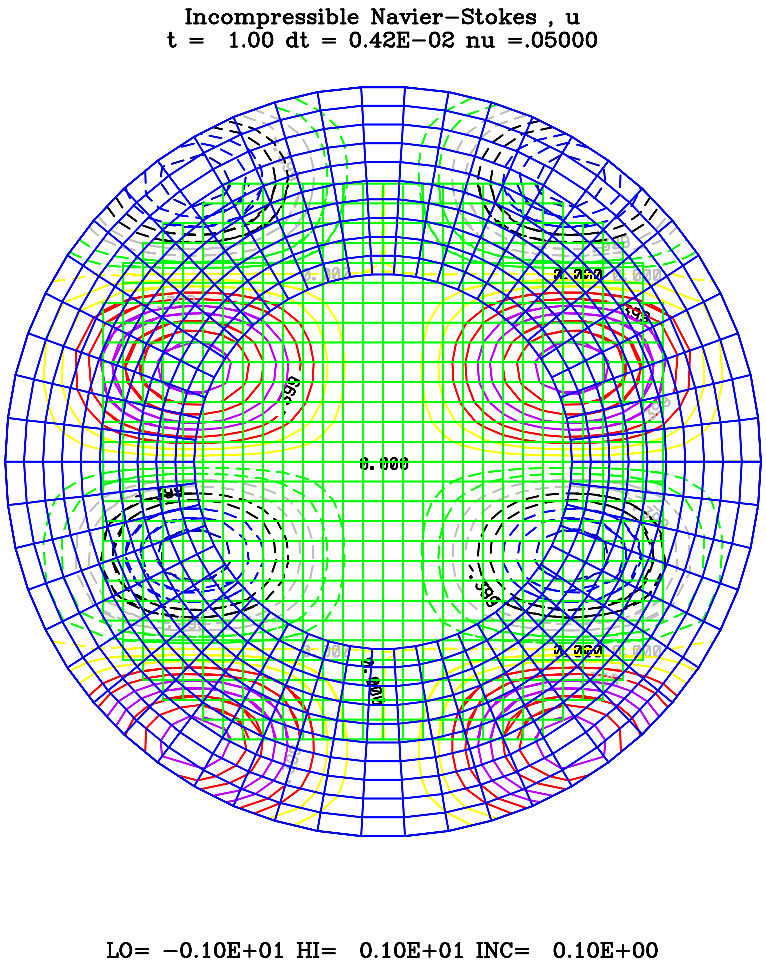

Figure 1: Flow in a circle, overlapping grid and computed solution

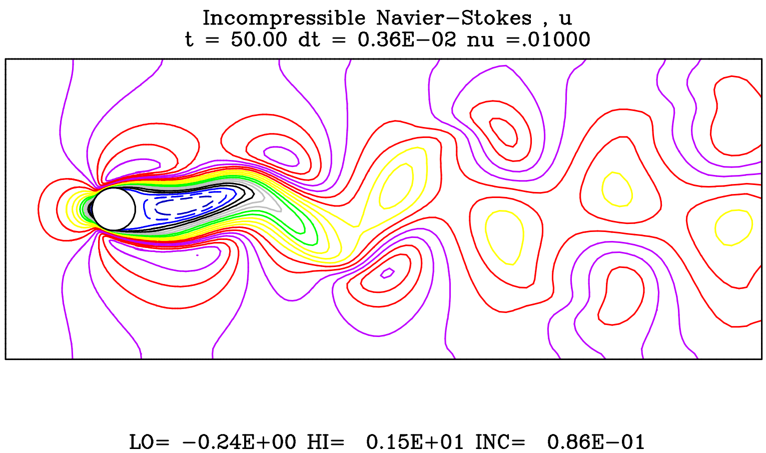

Figure 2: Flow past a cylinder, horizontal velocity

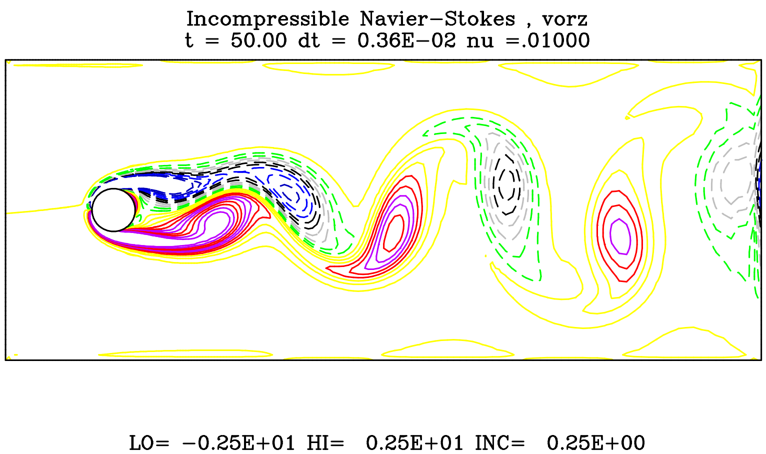

Figure 3: Flow past a cylinder, vorticity, max=26, min=−26.

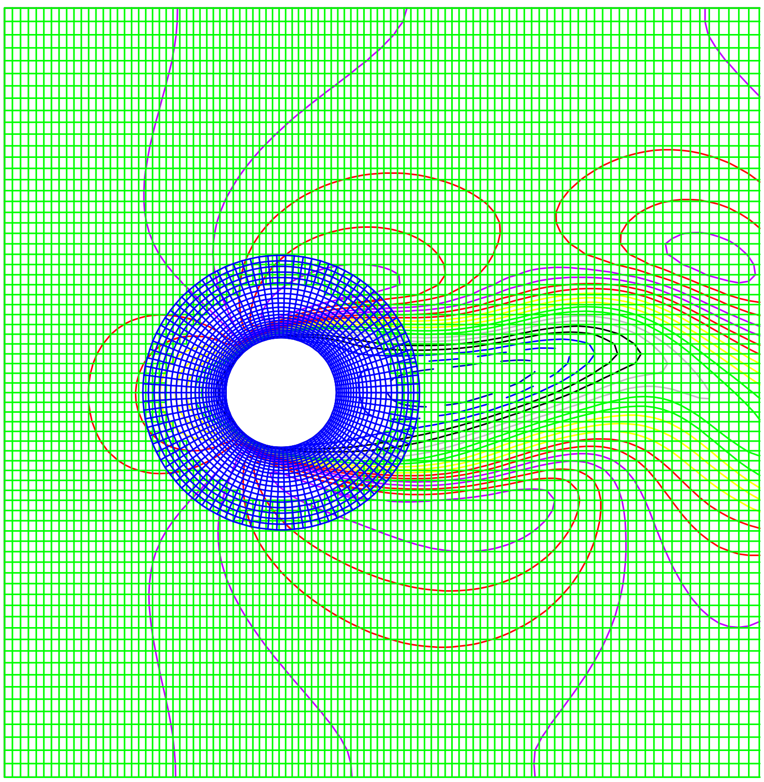

Figure 4: Overlapping grid near the cylinder with contours of u